Chapter 26
Use of Ground-Penetrating Radar to Determine Depth to Compacted Layer in Soils Under Pasture

Edwin Muñiz, Richard K. Shaw, Daniel Gimenez, Carey A. Williams and Laura Kenny

Abstract New Jersey, like many states in the northeastern USA, has a high demand for grazing land for horses. Grazing lands are often intensively used because of the limited possibilities for crop rotation. A ground-penetrating radar (GPR) study was conducted in an area under different management with soils formed in old alluvium and fluviomarine sediments (Ultisols). In the grazing field, no significant signs of compaction were detected with GPR. In the feeding fields, compaction was significant within 24 cm soil from the soil surface. The GPR data were used to generate a contour map representing the depth to the compacted layer. It is concluded that soil compaction can be adequately mapped using GPR.

Keywords GPR · Soil compaction · Grazing land

26.1 Introduction

Ground-penetrating radar (GPR) is a noninvasive technology for the study of the subsurface soil features (De Benedetto et al. 2013). GPR has been effectively used in a range of investigations, including locating burials (Miller 1996), underground utilities (Cheng et al. 2013), and assessing soil properties (Doolittle and Butnor 2008). This technology complements traditional and more labor-intensive method of collecting field data and can provide a continuous image of the soil subsurface (Doolittle and Butnor 2008; Paterson and Laker 1996). Freeland et al. (1998)

E. Muñiz (✉) · R.K. Shaw
United States Department of Agriculture, Natural Resources Conservation Service, Somerset, NJ, USA
e-mail: Edwin.Muniz@nj.usda.gov

D. Gimenez · C.A. Williams · L. Kenny
Rutgers, The State University of New Jersey, New Brunswick, NJ, USA

utilized the continuous profiling capabilities of GPR to determine soil horizons, depth to bedrock, preferential flow paths, and differentiate soil parent materials. Petersen et al. (2006) used GPR to identify variations in soil compaction and soil texture. They demonstrated the use of GPR to identify areas of loamy soils with high risk for soil compaction compared to areas of sandy soils where the risks for soil compaction are lower.

Soil compaction exerts a negative impact on soil productivity as it reduces pore spaces and decreases gas exchange, reduces water and root movement, and increases soil bulk density. New Jersey, like many states in the northeastern USA, has a high demand for grazing land. The equine industry ranks number 8 in sales value by agricultural commodity statewide and 26th in the USA (USDA NASS 2014). The equine industry generates substantial revenues, and the land is often intensively used, and in many instances, soils are compacted. Soil compaction poses a serious threat to pasture quality and nutritional value and a potential threat to surface water quality by runoff. GPR could be a quick and effective technology to assess soil compaction.

The objectives of this study were to (1) compare the effectiveness of a 400 MHz and 900 MHz GPR antenna to identify compacted soil layers and (2) generate a map showing depth to compacted layer that can be used for planning and implementation of best management practices.

26.2 Materials and Methods

26.2.1 The Study Site

The study was conducted at the Equine Research Farm located in the Rutgers Agricultural Research Farm (40°28′16″N, 74°25′42″W) in New Brunswick, New Jersey, USA. The study area is approximately 6.6 ha and consists mostly of grazing land, with a mix of good standing pasture, and areas used for feeding where the horses concentrate. The study area is located in a transition zone between two soils. The area is mapped as Nixon and Fallsington soil series with a Soil Taxonomic Classification of fine-loamy, mixed, semiactive, mesic Typic Hapludults and fine-loamy, mixed, active, mesic Typic Endoaquults, respectively (Soil Survey Staff 1999), or Haplic Acrisols and Stagnic Acrisols according to the World Reference Base (IUSS Working Group WRB 2014). Nixon is formed in old alluvium with a moderate permeability in the solum, very deep to bedrock (>150 cm), seasonal high water table exceeding 102 cm, and an extremely acid to strongly acid soil reaction. Fallsington is formed in fluviomarine sediments with a moderately high permeability in the solum, very deep to bedrock, seasonal high water table from the soil

surface to 30 cm, and an extremely acid to strongly acid soil reaction. The geology in the area is dominated by Lower Paleozoic to Precambrian sediments and igneous rocks that have been metamorphosed in the eastern part and crustal trough or basin in the central part from the Triassic period (USDA-NRCS 2006). The average annual precipitation in the area is 746–1645 mm (ONJSC 2014) with a maximum precipitation as high-intensity and convective thunderstorms in spring and early in summer.

26.2.2   GPR Readings

The effectiveness of a 400 and 900 MHz antennas to detect compacted layers were compared on two plots of 2.8 m^2 with different pasture quality (Fig. 26.1). Plot 1 was mostly grazing land with a mix of good standing pasture on Fallsington soil, and Plot 2 was an area used for feeding where the horses concentrate with pasture in

Fig. 26.1 Location of Plots 1 and 2 showing the grassland quality and position in the landscape

poor condition on the Nixon soil. Field data were collected in two small soil pits (30 cm soil depth) to compare with the GPR scans by matching the high dielectric signals from the GPR to the zones with root-restrictive layers identified by visual inspection.

The study was expanded across a 6.6 ha area that was divided into 16 plots of different shapes and sizes for prescribe grazing management. Data were collected with the GPR in a zigzag pattern with a north–south alignment and an average spacing of 8 m. In addition, field data were collected randomly throughout the area by digging small soil pits and describing depth to compacted layer. The data were used to validate the information obtained from GPR.

The GPR system used was the TerraSIRch Subsurface Interface Radar (SIR) System-3000 and the 400 and 900 MHz antennas manufactured by Geophysical Survey Systems, Inc. This GPR system was mounted on a standard survey cart with an integrated survey wheel encoder and georeferenced with the Garmin Global Positioning System Map 76 receiver. The 400 and 900 MHz antennas are shielded with a maximum depth in optimum soil conditions (dry, sandy, low electrical conductivity) from 4 to 1 m, respectively. The instrument was calibrated over a known buried metal object as recommended by Zobeck et al. (1985). Equations (26.1) and (26.2) were used to estimate the velocity of propagation in the soil (v) and the dielectric permittivity (Er) of the soil. These parameters were used to convert the two-way travel time of the propagated radar energy into a depth scale.

$$v = \frac{2 \times D}{t} \tag{26.1}$$

where v is the velocity of propagation in the soil (m/ns), D is the depth of penetration of the radar wave to a known object (m), t is the travel time (ns), and

$$Er = \left(\frac{c}{v}\right)^2 \tag{26.2}$$

where c is the speed of light or 0.2998 m/ns. Velocity of propagation and dielectric permittivity were used to convert the two-way travel time of the propagated radar energy into a depth scale.

The data were processed in RADAN 7 (GSSI 2012) by editing the initial positioning time zero, horizontal high, and low pass filtration, with background noise removal for the purpose of improving the resolution and interpretations of the compacted layers. The interpreted radar data (presence and depth to compacted layer) were used to generate a contour map in ArcMap (ESRI 2013). A polygon-type map was created by linear kriging and using the mean for duplicated positions in a simple type without data transformation and creating a contour map with depth to the compacted layer.

26.3 Results and Discussion

The 400 MHz antenna provided greater signal penetration than the 900 MHz antenna. However, signal scattering was severe with the 400 MHz antennas due to the presence of both a relatively high moisture content associated with the seasonal high water table (Fig. 26.2) and an argillic horizon with clay content ranging between 18 and 25 % (Fig. 26.3). Even though the signal penetration extended to a depth between 125 and 200 cm, soil features were not well defined and were masked by the signal noise.

The 900 MHz antenna provided slightly improved imagery of the subsurface (Figs. 26.4 and 26.5), even with a more noticeable amount of coarse fragments found in the Nixon soil (Fig. 26.6). In plot 1, with good standing pasture, no soil
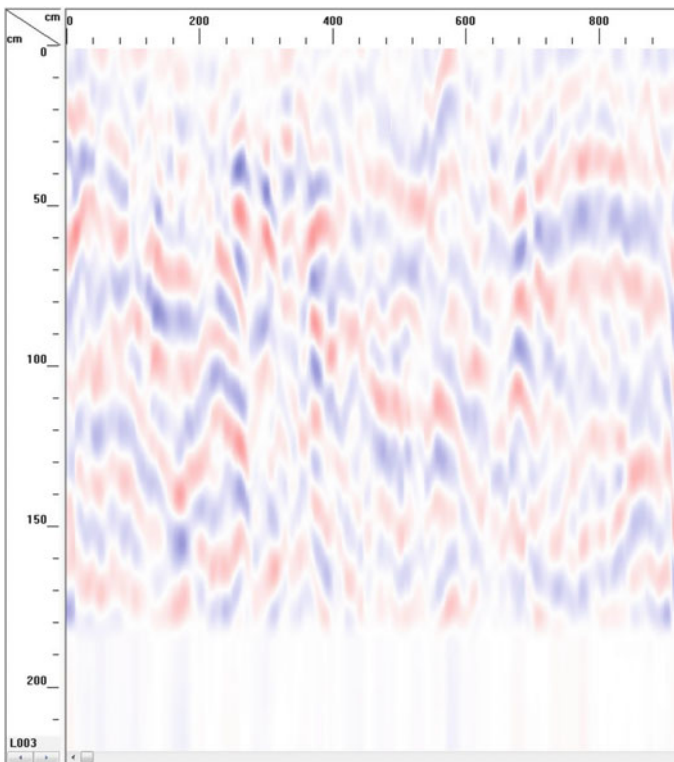

Fig. 26.2 Plot 1 400 MHz showing high reflectance as a result of a seasonal high water table. Horizontal and vertical scales are in cm
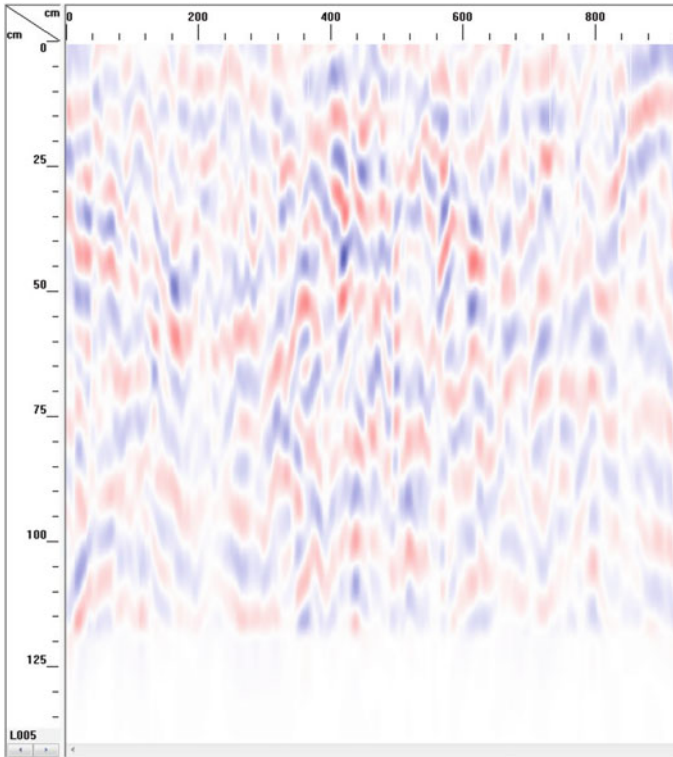
Fig. 26.3 Plot 2 400 MHz GPR readings showing high reflectance as a result of clay increase in the soil profile. Horizontal and vertical scales are in cm

compaction was detected with the exception of a very thin layer with platy soil structure that showed a higher dielectric near the surface. In addition, this soil had a higher moisture content compared to plot 2. Plot 1 was located in a lower position in the landscape and was likely less accessed by the horses due to its wetness. In plot 2, soil compaction was detected ranging in depth from 0 to 24 cm; this area included watering and feeding facilities in addition to the animal shelter. The compaction could also be associated with mechanical activities following reseeding of the pasture. Field observations detected a decrease in root abundance, distribution, and size between the Ap2 and Bt horizons (Fig. 26.6), thus supporting the interpretations from the GPR scan.
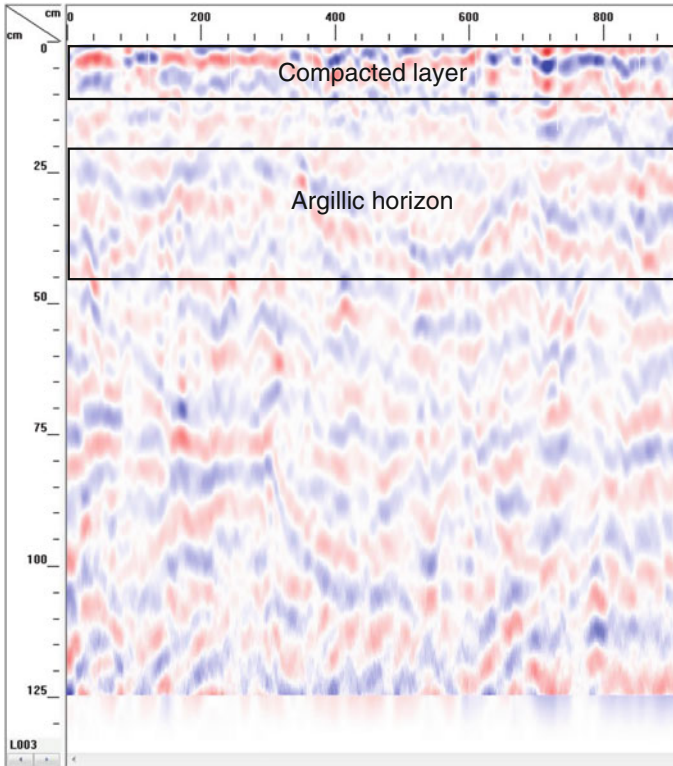
Fig. 26.4 Plot 1 900 MHz GPR reading showing a thin compacted layer and an argillic horizon. Horizontal and vertical scales are in cm

For the second part of the project, the data for the entire field showed an average depth of 8.7 cm to the top of a compacted layer (Table 26.1). A map was generated with the distribution of the depth to the compacted layer in 8-cm increments in relation to the topography (Fig. 26.7), which shows the general relationship between a higher dielectric and topography. With flat to slightly rolling topography, a discontinuous compacted layer at the soil surface was found over the argillic horizon, which began at about 24 cm in depth (Fig. 26.8). This topography is typical for an area that is wet for a prolonged time, with limited traffic, and also corresponds to the narrow corridor used to move the horses during the field rotation.
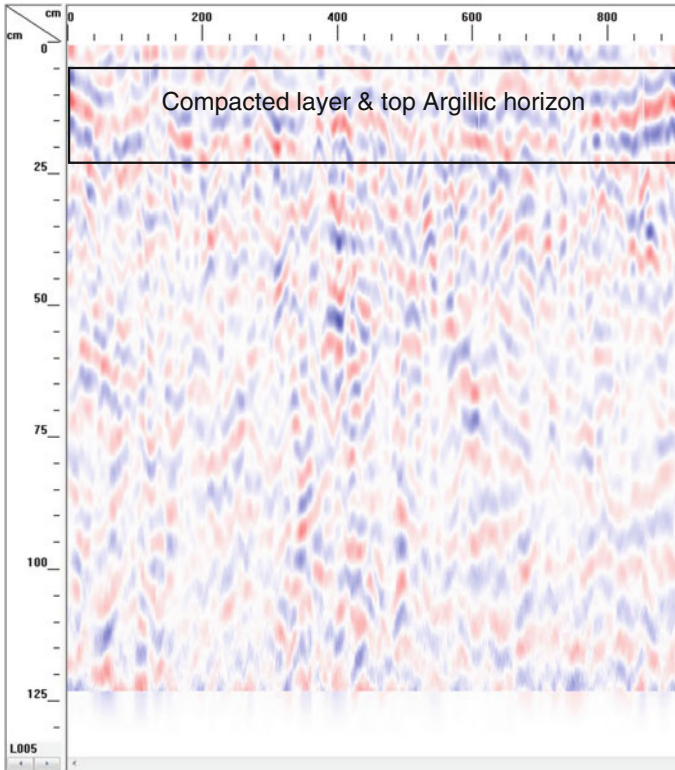
Fig. 26.5 Plot 2 900 MHz GPR reading showing compacted layer between 5 and 24 cm from the soil surface. Horizontal and vertical scales are in cm

Fig. 26.6 Nixon soil profile for Plot 2 showing an increase in coarse fragments starting around 10 cm, an argillic horizon around 20 cm, and a decrease in root abundance, distribution, and size starting around 10 cm

Table 26.1 Descriptive statistics for the depth to compaction over the entire field detected with GPR

Depth (cm)	
Mean	8.7
Standard error	0.0128
Median	4.6
Mode	0
Standard deviation	10.6708
Sample variance	113.8666
Kurtosis	1.1645
Skewness	1.2933
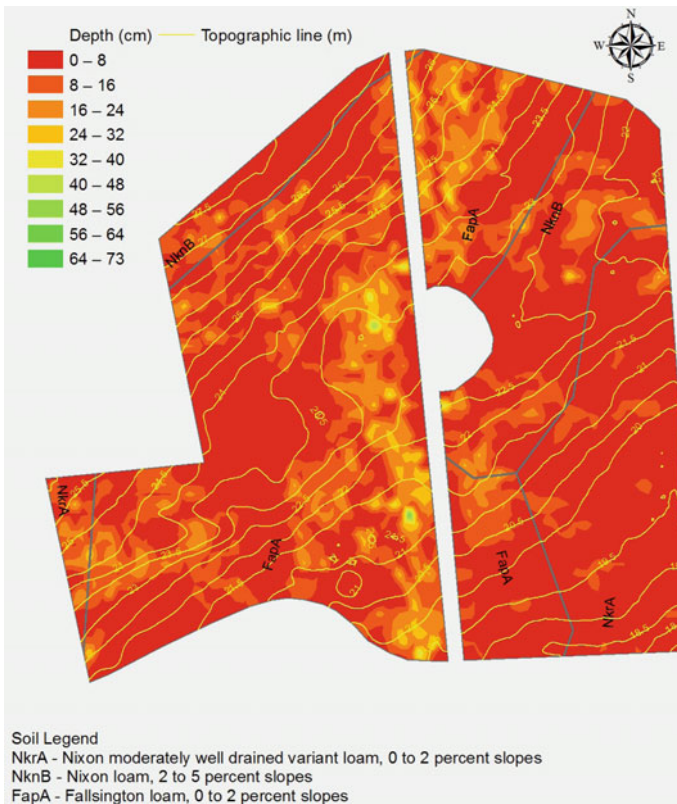
Fig. 26.7 Compacted zone distribution map generated using kriging. Showing depth to soil compaction in cm interpreted from the GPR
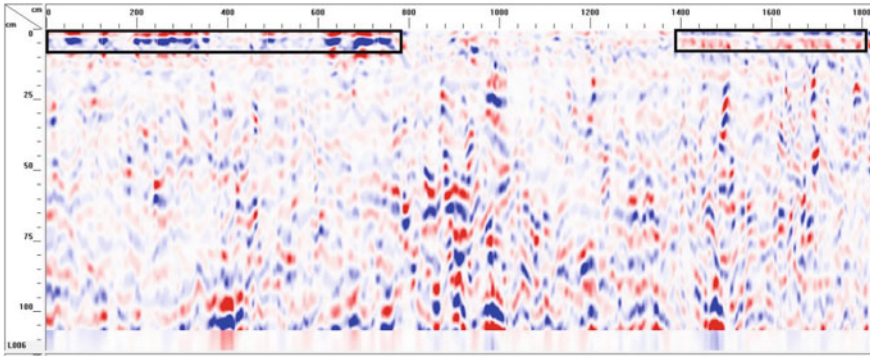
Fig. 26.8 Zone with discontinuous compacted layer with a high dielectric

26.4 Conclusions

In combination with field verification, ground-penetrating radar (GPR) is a valuable and diverse tool in the soil scientist's toolbox with the potential to be used in locating problematic areas and identifying the extent of soil compaction. In this investigation, results of the GPR correlated with the observations made in soil pits. Since GPR data do not provide information on the degree of soil compaction, calibration would be needed to use as a survey tool.

References

Cheng NF, Conrad Tang HW, Chan CT (2013) Identification and positioning of underground utilities using ground penetrating radar (GPR). Sustainable Environ Res 23(2):141–152

De Benedetto D, Castrignano A, Rinaldi M, Ruggieri S, Santoro F, Figorito B, Gualano S, Diacono M, Tamborrino R (2013) An approach for delineating homogeneous zones by using multi-sensor data. Geoderma 199:117–127

Doolittle JA, Butnor JR (2008) Chapter 6, soils, peatlands, and biomonitoring. 179–202 pp. In: Jol HM (ed) Ground penetrating radar: theory and applications. Elsevier, Amsterdam, The Netherlands

ESRI (2013) ArcGIS 10.2 for desktop: version 10.2.0.3348. Redlands, Environmental Systems Research Institute, CA

Freeland RS, Yoder RE, Ammons JT (1998) Mapping shallow underground features that influence site-specific agricultural production. J Appl Geophys 40:19–27

GSSI (2012) Radar data analyzer for windows: version 7.4.14.1113. Nashua, NH

IUSS Working Group WRB (2014) World reference base for soil resources 2014. International soil classification system for naming soils and creating legends for soil maps. World Soil Resources Reports No. 106. FAO, Rome

Miller PS (1996) Disturbances in the soil: finding buried bodies and other evidence using ground penetrating radar. J Forensic Sci 41(4):648–652

ONJSC (2014) New Jersey Agricultural Experiment Station. Northern New Jersey monthly precipitation. Available at: http://climate.rutgers.edu/stateclim/

Paterson DG, Laker MC (1996) Using ground penetrating radar to investigate spoil layers in rehabilitated minesoils. S Afr J Plant Soil 16(3):131–134

Petersen H, Fleige H, Rabbel W, Horn R (2006) Geophysical methods for imaging soil compaction and variability of soil texture on farm land. Adv Geol 38:261–272

Soil Survey Staff (1999) Soil taxonomy: a basic system of soil classification for making and interpreting soil surveys. 2nd edn. Natural resources conservation service. U.S. department of agriculture handbook 436

USDA NASS (2014) Census of agriculture. Available at: www.nass.usda.gov/

USDA-NRCS (2006). Land Resource regions and major land resource areas of the United States, the Caribbean, and the Pacific Basin. U.S. Department of Agriculture Handbook 296

Zobeck TM, Lyon JG, Mapes DR, Ritchie A Jr (1985) Calibrating ground penetrating radar data for soil applications. Soil Sci Soc Am J 49:1587–1590